Biochemical and Biophysical Research Communications 464 (2015) 929–935

Contents lists available at ScienceDirect

Biochemical and Biophysical Research Communications

journal homepage: www.elsevier.com/locate/ybbrc

Structural and functional analyses of nucleosome complexes with mouse histone variants TH2a and TH2b, involved in reprogramming

Sivaraman Padavattan [a], Toshie Shinagawa [b], Kazuya Hasegawa [c], Takashi Kumasaka [c], Shunsuke Ishii [b], Thirumananseri Kumarevel [a, d, *]

[a] RIKEN SPring-8 Center, Harima Institute, 1-1-1 Kouto, Sayo, Hyogo 679-5148, Japan
[b] Laboratory of Molecular Genetics, CREST Research Project of JST (Japan Science and Technology Agency), RIKEN Tsukuba Institute, 3-1-1 Koyadai, Tsukuba, Ibaraki 305-0074, Japan
[c] Japan Synchrotron Radiation Research Institute (SPring-8), 1-1-1 Kouto, Sayo-cho, Sayo-kun, Hyogo 679-5198, Japan
[d] Structural Biology Laboratory, RIKEN Yokohama Institute, 1-7-22 Suehiro-cho, Tsurumi, Yokohama, Kanagawa 230-0045, Japan

ARTICLE INFO

Article history:
Received 24 June 2015
Accepted 14 July 2015
Available online 17 July 2015

Keywords:
TH2a
TH2b
Histone variants
Chromatin
Reprogramming

ABSTRACT

Histone variants TH2a and TH2b are highly expressed in testes, oocytes and zygotes. Our recent analysis suggested that these histone variants enhance the induced generation of pluripotent stem cells (iPSCs) when co-expressed along with four transcription factors, Oct3/4, Sox2, Klf4 and c-Myc (OSKM), and are associated with an open chromatin structure [1]. In the present study, we report the crystal structures of nucleosomes (NCPs) with the mouse histone variants, TH2a and TH2b. The structures revealed two significant changes, as compared to the canonical counterparts: fewer histone-DNA contacts and changes in dimer–dimer interactions between TH2a-TH2a′ (L1-loop). I*n vivo* studies with domain swapping and point mutants of the variants revealed that the residues in the histone tails and the TH2a-L1 loop are important for reprogramming. Taken together, our work indicates that the NCP variants with structural modifications and flexible tails are most likely important for enhanced reprogramming of functions.

1. Introduction

During spermatogenesis, chromatin restructuring occurs by the exchange of somatic histones with testis-specific histone variants [2–4]. TH2a and TH2b were originally identified as testis-specific histone variants [5–8] and they share a promoter, suggestive of a common function [9]. Our recent study showed that both variants are also expressed in oocytes and fertilized eggs, and their expression levels decreased as the embryos differentiated into blastocysts. The TH2a/TH2b variants induce an open chromatin structure, and are enriched, and uniformly distributed both on the X chromosomes and autosomes [1].

Chromatin decondensation is a hallmark of reprogramming [10,11]. Somatic cells can be experimentally reprogrammed back to pluripotency by nuclear transfer into oocytes [12], fusion with embryonic stem (ES) cells [13] or artificially overexpressing four transcription factors, Oct3/4, Sox2, Klf4 and c-Myc (OSKM) [14]. Our recent study revealed that the histone variants TH2a and TH2b, when co-expressed with OSKM, enhanced the generation of iPSCs by nine-fold. However, either TH2a or TH2b expressed together with canonical H2a/H2b had no effect on reprogramming [1]. Nucleoplasmin (Npm) is an abundant oocyte protein that plays an important role in chromatin decondensation during fertilization [15], and its activity is modulated through phosphorylation [16]. When phosphorylation mimics of nucleoplasmin (P-Npm) and TH2a/TH2b were coexpressed, they enhanced the OSKM-induced iPSC generation by 18-fold. Moreover, iPSCs were generated using only Klf4 and Oct3/4 coexpressed with TH2a/TH2b and P-Npm [1].

Histone variants and chemical modifications of histones and DNA generate diversity in chromatin structure and function [4,17]. In this study, we have determined the nucleosome structures with the mouse testis-specific histone variants TH2a and TH2b, to identify the structural differences as compared to their canonical counterparts. The *in vivo* studies with domain swapping and point mutants of the histone variants revealed the regions and the key residues important for the reprogramming function.

* Corresponding author. Structural Biology Laboratory, RIKEN Yokohama Institute, 1-7-22 Suehiro-cho, Tsurumi, Yokohama, Kanagawa 230-0045, Japan.
E-mail address: kumarevel.thirumananseri@riken.jp (T. Kumarevel).

http://dx.doi.org/10.1016/j.bbrc.2015.07.070
0006-291X/

2. Materials and methods

2.1. Histone expression and purification

The mouse testis-specific histone variants, TH2a and TH2b, and the canonical human histones, H2a, H2b, H3.1 and H4, were over-expressed in *Escherichia coli* and purified according to the previously published protocols [18,19]. The domain-swapped and point mutant histone variant proteins were purified in a similar manner.

2.2. Nucleosome preparation and crystallization

The 146-bp DNA and the NCPs were prepared as described previously [19,20]. The octamers were separated from the excess dimers by gel-filtration chromatography in a buffer containing 2 M NaCl. The nucleosomes were reconstituted by salt dialysis and purified from the excess DNA by ion exchange chromatography (Mono-Q 5/5 column, GE Healthcare). Nucleosomes were concentrated to 3.5–4 mg/mL and crystallized by the hanging drop method under the following conditions: 20 mM potassium cacodylate, pH 6.0, 60–70 mM KCl and 70–90 mM $MnCl_2$. The crystals were cryo-protected with the mother liquor, containing with 24% 2-methyl-2,4-pentanediol (MPD) and 6% trehalose.

2.3. Data collection and structure determination

Diffraction data were collected using the synchrotron radiation source at the Beamline BL41XU Station of SPring-8, Japan. The NCP crystals belonged to the orthorhombic space group $P2_12_12_1$, with one molecule per asymmetric unit. The structures were solved by the molecular replacement method, with the PDB entry 1AOI as a search model [21], using the Phaser program. The refinement was performed with Refmac [22] and CNS [23], and model building was accomplished with Coot [24] and Quanta (Accelrys, San Diego, CA, USA). The data collection parameters and refinement statistics are provided in Table S1. All of the structure figures were produced using PyMOL. The atomic coordinates of the GCH, GCHV1, GCHV2 and canonical NCPs have been deposited, with the RCSB ID codes 3X1T, 3X1U, 3X1V and 3X1S, respectively.

2.4. Domain swapping, point mutations, iPSC generation and FACS analysis

The details of the procedures related to domain swapping, point mutations, iPSC generation and FACS analysis are explained in Supplementary Materials and Methods section.

3. Results and discussion

3.1. Nucleosome structures with mouse TH2a and TH2b variants

The histone variants TH2a and TH2b are abundantly expressed during spermatogenesis [2,3], as well as in oocytes and fertilized eggs [1]. Knockout studies in mice revealed that female homozygous *TH2a*$^{-/-}$*TH2b*$^{-/-}$ oocytes have reduced capacity for embryogenesis, and both variants contribute to paternal genome activation [1]. TH2a and TH2b share 87% and 85% sequence identities with the mouse canonical H2a and H2b, respectively (Fig. 1A). Most of the non-conserved residues in the variants are localized at the N- and C-terminal histone tail regions and within the TH2a-L1 loop.

We have determined the structures of three nucleosome core particles (NCPs) with mouse TH2a and TH2b variants: GCH (TH2a-TH2b-H3-H4)$_2$, and the cross variants GCHV1 (TH2a-H2b-H3-H4)$_2$ and GCHV2 (H2a-TH2b-H3-H4)$_2$, with 146-bp palindromic DNA derived from human α-satellite DNA, by the molecular replacement method (Fig. 1B). (Note: we used the human canonical histones H2a, H2b, H3 and H4, along with the mouse TH2a and TH2b for the nucleosome preparation. The Human and Mouse canonical histones H2a and H2b are having almost 99% sequence identity; H3 and H4 are having 100% identity between the species). In addition, we determined the structure of the human canonical nucleosome, for comparison. The data collection and refinement statistics are summarized in Table 1. Unlike the testis-specific H3T variant [25], the TH2a and TH2b variants form stable octamers under high salt concentrations. The superposition of the GCH, GCHV1, and GCHV2 nucleosomes with the canonical-NCP gave root mean square deviations (r.m.s.d.) of 0.3 Å, 0.5 Å and 0.37 Å, respectively. Intriguingly, closer inspections of the variant NCPs (GCH, GCHV1, and GCHV2) revealed two changes: fewer histone-DNA contacts and significant changes in the L1-L1′ loop interactions between the TH2a-TH2a′ dimers. Recently, chromatin structure containing the human histone H2B variant TSH2B was reported and the overall structural composition is similar to our GCHV1 [26].

3.2. Histone-DNA interactions

The NCP containing the TH2a and TH2b variants had fewer histone dimer-DNA contacts, as compared to its canonical counterpart, due to the altered side-chain conformations of the DNA-interacting residues. In the canonical-NCP, the H2a/H2a′-Arg21 side-chain forms strong H-bonding interactions with DNA at ±31-bp from the entry/exit sites, and also forms H-bonds with the H2a/H2a′-Lys16 main chain CO, thereby holding the H2a N-terminal tail (Fig. 2). Intriguingly in GCH-NCP, the TH2a/TH2a′-Arg21 side chain conformation is altered, resulting in the loss of interactions with DNA and the TH2a/TH2a′-Lys16 residue, and the formation of the two new H-bonds with the TH2b C-terminal end. In the cross variant GCHV2-NCP, the H2a/H2a′-Arg21 side-chain forms H-bonds with the TH2b C-terminus, and weakly associates with DNA and the H2a/H2a′-Lys16 residue. In GCHV1-NCP, the side-chain density of Arg21 was undetectable, presumably due to the high b-factors around the region when compared to other structures.

Single molecule studies revealed that the histone-DNA interactions are unevenly distributed within the nucleosomes. The nucleosome dyad has the strongest interactions, and these are followed by two regions localized approximately ±33-bp from the nucleosome entry/exit sites [27]. Interestingly, the DNA contacts lost at ±31-bp from the entry/exit sites in our variant NCPs might have effects on the nucleosomal stability and function. Histone variants generate diversity in chromatin structures and functions by altering the properties of the nucleosomes [17]. Biochemical analysis suggests that hTSH2B induces the octamer instability compared to H2B [28]. Further studies using mutant mice lacking the expression of TH2B suggest that it not only compensates expression of H2B during spermatogenesis but also it affects the epigenetic reprogramming through histone-DNA or histone–histone interactions [29]. Very recent data clearly indicated that lacking both the TH2A and TH2B variants affects in spermatogenesis by disturbing cohesion release and histone replacement [30]. In the *sin* mutant, the mutated residues encircling the nucleosome dyad, where H3–H4 pair with each other, affect the nucleosome stability, and thereby enhance the octamer mobility with respect to the DNA [31]. The H3 homologue CENP-A has been shown to affect the binding of a 13-bp DNA fragment at the NCP entry/exit sites [32]. The human testis-specific H3T affects nucleosome stability, due to the weaker association of the (H3T-H4)$_2$ tetramer with the H2a-H2b dimer, without affecting the interaction with DNA [25].

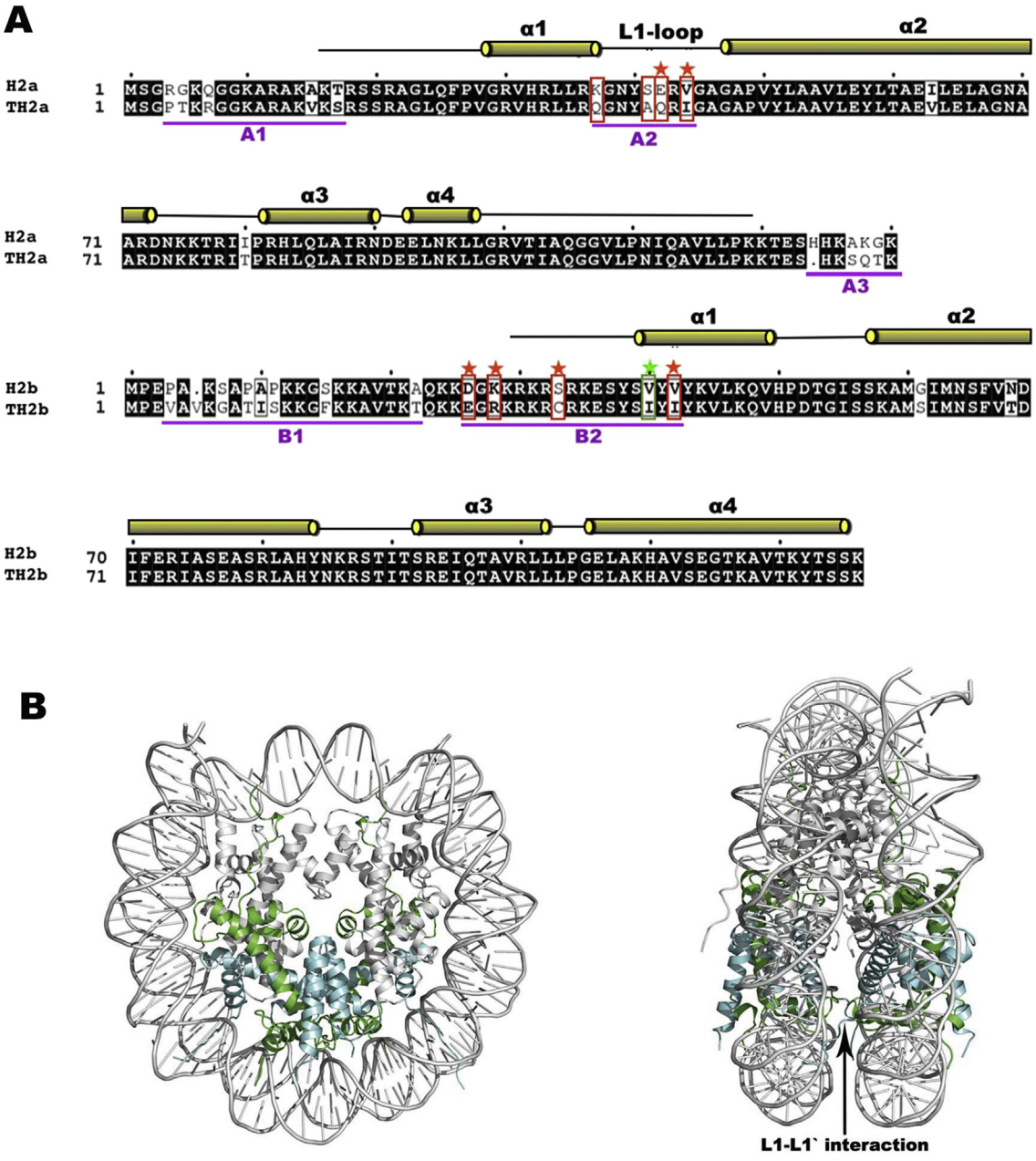

Fig. 1. Sequence alignment and nucleosome structure. A) The sequences of the histone variants, TH2a and TH2b, were aligned with those of the mouse canonical H2a and H2b. Schematic representations of secondary structures are shown above the alignment, and the TH2a L1-loop is labeled. The residues underlined in magenta were domain-swapped with the corresponding canonical sequences, and are labeled A1, A2 and A3 for TH2a, and B1 and B2 for TH2b. The residues enclosed in red boxes within the TH2a (A2) and TH2b (B2) domains were substituted by point mutations with the corresponding canonical residues. The residues marked with red stars down-regulate iPSC generation. The residue in the green box with a star up-regulates iPSC generation by two-fold. B) Crystal structure of the nucleosome complex GCH-NCP (TH2a-TH2b-H3-H4), with TH2a (cyan) and TH2b (green) highlighted. The left figure is rotated by 90° along the Y-axis, and the TH2a-TH2a′ interaction between the L1-L1′ loops is marked by an arrow. (For interpretation of the references to colour in this figure legend, the reader is referred to the web version of this article.)

3.3. *L1-L1′ loop interactions*

In nucleosomes, the L1-loop connecting the H2a α1-α2 helixes is the only site of contact between the H2a-H2b dimers, and it mediates the interactions between H2a-H2a′ [21]. The L1-loop region is a major site of sequence variation within a histone fold [33] among the H2a variants, and it has been suggested to play a role in the cooperative incorporation of a second dimer during NCP assembly [34].

In the canonical NCP the L1-L1′ loop interface interactions are stabilized by the H2b-His83 residues, which are located on both sides of the L1-L1′ interfaces and form H-bond contacts (Fig. 3A–D). In GCH-NCP, the L1-L1′ interface lacks H-bond contacts. Intriguingly, the side-chain dihedral angle for TH2b-His84, in both dimers with well-defined electron density, changed its conformation as compared to the canonical H2b. This change affects the interactions between the His84 side-chain and the L1-L1′ interface, and shifts the position of TH2a-Asn39 towards the space generated by the TH2b-His84 residue. In the cross variant GCHV1-NCP, the H2b-His83 side-chain adopts a conformation similar to that in GCH, and thus has lost the contact with the interface. Also, it is noteworthy to mention that we did not observe any structural changes

Table 1
Data collection and refinement statistics.

Data collection	GCH	GCHV1	GCHV2	Canonical
Wavelength	1.00	1.00	1.00	1.00
Space group	$P2_12_12_1$	$P2_12_12_1$	$P2_12_12_1$	$P2_12_12_1$
Cell dimensions				
a, b, c (Å)	105.77,109.59, 181.59	104.43,109.18,175.00	99.32, 108.47,168.67	105.38, 109.36,175.57
α, β, γ (°)	90, 90, 90	90, 90, 90	90, 90, 90	90, 90, 90
Resolution (Å)	2.80 (2.90-2.80)	3.25 (3.31-3.25)	2.90 (3.00-2.90)	2.80 (2.90-2.80)
Reflections (unique)	51,865 (5066)	32,890 (1638)	38,723 (3737)	46,322 (3349)
I/sigma I	19 (2.04)	24.5 (2.65)	13.26 (2.05)	21 (1.76)
Completeness (%)	99.6 (99.1)	99.9 (100)	96.8 (95.3)	91.9 (67.9)
Redundancy	8.1 (7.1)	13.8 (14.0)	11.4 (10.1)	9.8 (8.3)
Rmerge	0.128 (0.72)	0.138 (0.78)	0.184 (0.74)	0.097 (0.73)
Refinement				
*R*work/Rfree	0.203/0.266	0.199/0.270	0.191/0.258	0.190/0.258
Number of atoms				
Protein	6201	6157	6417	5956
DNA	5980	5980	5972	5980
Water	107	30	–	57
B–factors (Å^2)				
Protein	44.7	83.8	27.9	61.5
DNA	100.6	142	63	121.6
R.m.s deviations				
Bond lengths (Å)	0.008	0.009	0.009	0.009
Bond angles (°)	1.419	1.423	1.565	1.436
Ramachandran plot				
Favored (%)	99	96.95	98.68	97.82
Allowed (%)	1.6	2.92	1.32	2.04
Outliers (%)	0.4	0.13	–	0.14
PDB Code	3X1T	3X1U	3X1V	3X1S

around the residue Asn84 (Ser85 in TSH2B) of TH2B in GCH or GHV2 nucleosome structures, when compared to TSH2B [26]. In GCHV2-NCP, the L1-L1′ interface has three H-bonds and resembles the canonical-NCP. Thus, the overall L1-L1′ loop interactions in the canonical and GCHV2-NCPs are tightly connected, as compared to those in GCH and GCHV1, and the following changes could be due to the Ile substitution of Val44 in the TH2a L1-loop.

In comparison to the NCPs described above, the other H2a variant NCPs have markedly different L1-L1′ loop conformations and interactions (Fig. 4). In H2a.Z-NCP, the L1-L1′ loop interaction between H2a.Z-H2a.Z′ is extensive, and the path of the α1-helix and parts of the loop connecting the α1 and α2-helixes differ from those of the canonical structure [35]. In the macroH2a-NCP, the L1-L1′ interface is less flexible and has more hydrophobic interactions. The Lys40 side chain is sandwiched between Tyr41 and Pro39′ and *vice versa* [34]. It is interesting to note that the H2b-His79 residue in both the H2a.Z- and macroH2a-NCPs does not interact with the L1-L1′ interface, and adopts a similar conformation to GCH.

3.4. TH2a/TH2b domain swapping and iPSC generation

Histone tails are epigenetically modified and regulate distinct transcriptional states and nuclear events [36], and are essential for the formation of highly ordered structures [37]. The mouse TH2a/TH2b variants enhance OSKM-induced reprogramming. However, neither each individual TH2a/TH2b variant nor the canonical H2a-H2b has the capacity for enhancing iPSC generation [1]. The above studies clearly suggested that the functional residues in the flexible N- and C-terminal tails and the coexistence of TH2a-TH2b have determining roles in reprogramming. Moreover, the structural studies with these variants revealed changes in the L1-L1′interface and fewer histone-DNA interactions within the nucleosome. To understand the significance of the histone tails and the structural changes of the nucleosome in iPSC generation, we performed domain swapping of variants with mouse canonical histones, as depicted in Fig. 1A. Three domain swaps for TH2a, corresponding to the N-terminal region (A1), the L1-loop (A2) and the C-terminus (A3), and two domain swaps (B1 and B2) for the N-terminus of TH2b were constructed. All five domain-swapping constructs were analyzed for their roles in iPSC generation.

The domain-swapped variants, along with the appropriate counterpart plus KOSM and P-Npm, were expressed in mouse embryonic fibroblasts (MEFs), which also express the GFP marker from the promoter of the ES cell-specific gene *Nanog*. The iPSC generation was analyzed by FACS (Supplementary Figure S1, A). The results clearly showed that all five domains are indeed important for iPSC generation. The swapped TH2a-L1 loop caused reduced iPSC generation, clearly signifying the importance of the structural changes at the L1-L1′interface. A closer view of the other four domains (A1, A3, B1 and B2) in the histone tail regions revealed changes in the positions of the functional residues. For example, the canonical H2b-Ser14 residue is phosphorylated by caspase-3-activated mammalian sterile twenty (Mst1) kinase, which plays an important role in regulating apoptotic chromosome condensation [38]. In TH2b, phenylalanine is located at the equivalent position, and is highly conserved among eukaryotic organisms (Supplementary Figure S1, B,C). Similarly, the H2a-Arg4 residue is deaminated by peptidylarginine deaminase 4 (PAD4), which represses gene transcription [39] and is replaced with Pro in TH2a. The N-terminal tail of H2b is known to be involved in chromatin condensation [40]. Also both of the H2A and H2B N-terminals are required for binding to the nuclear chaperones (Karyopherins family) to be imported into the nucleosome assembly machineries and the N-terminal deletion of H2B reduced its incorporation at all sites by approximately half due to the reduced protein stability though the overall function of H2B is intact in chromatin assembly [41,42], and these may be one probable reason why the N-terminal mutants of both the variants failed to reproduce the iPSC generation. Together, these results suggested that the variants of histone tails might establish alternative epigenetic marks as compared to the canonical counterparts, and they may affect the overall chromatin structure as well as iPSC reprogramming.

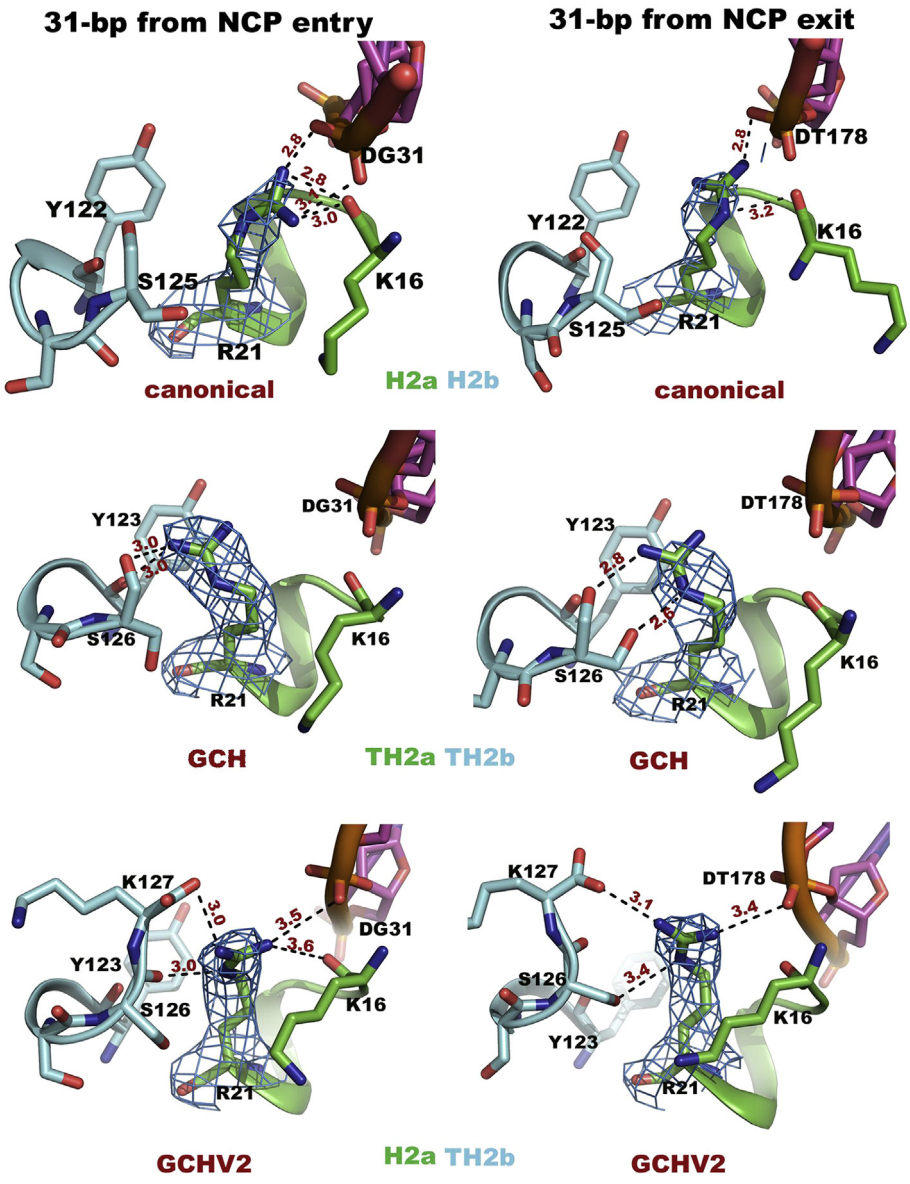

Fig. 2. Histone-DNA interactions. The Arg21/Arg21′ residues in TH2a/H2a from three nucleosome structures (GCH, GCHV2 and canonical-NCP) with 2Fo-Fc electron density maps contoured at 1.0σ are shown in a blue mesh, and their interactions with neighboring residues are depicted by dashed black lines with distances in red. (For interpretation of the references to colour in this figure legend, the reader is referred to the web version of this article.)

3.5. Point mutations in the TH2a (A2) and TH2b (B2) domains

The domain swapping studies clearly suggested that the histone tails and the structural changes in the dimer–dimer interactions between TH2a-TH2a′ (L1-loop) are important for iPSC generation. Among the five domains, only the TH2a-(A2) and TH2b-(B2) domains are structured within the NCP. To determine the importance of each non-conserved residue in the TH2a-(A2) and TH2b-(B2) domains, the residues shown in Fig. 1A were mutated to the corresponding canonical residues, and analyzed for their effects on reprogramming through a FACS analysis.

Intriguingly, two single amino acid substitutions in the TH2a-L1 loop, Gln42 to Glu and Ile44 to Val, each clearly affected the iPSC generation. The numbers of GFP^{+} cells with these mutants were significantly reduced (Supplementary Figure S1, D), while the Gln37 to Lys and Ala41 to Ser substitutions did not have a major effect. The crystal structure revealed that the L1-L1′ loop interaction in the NCP consists of both variants (GCH), and only with TH2a (GCHV1) lacks a H-bond, as compared to the H-bonding interaction seen with the canonical and GCHV2-NCPs. This clearly suggested that the replacement of Val44 with the bulky Ile residue in the TH2a L1-loop affects the interface interactions (Supplementary Figure S2, A).

The TH2b-(B2) domain has five non-conserved residues, and the point mutations of Glu27 to Asp, Arg29 to Lys, Cys34 to Ser and Ile43 to Val significantly reduced iPSC generation. Intriguingly, the TH2b-Ile41 to Val mutation up-regulated the iPSC generation by two-fold (Supplementary Figure S1, C-D). Furthermore, only the Ile41 and Ile43 residues had well-defined side chain densities and are strongly conserved among higher eukaryotic organisms (Supplementary Figure S1, C). In GCH-NCP, the TH2b-Ile43 residue is surrounded by a hydrophobic pocket and does not contact the DNA. By contrast, TH2b-Ile41 makes a hydrophobic contact with the DNA at ±25-bp from the

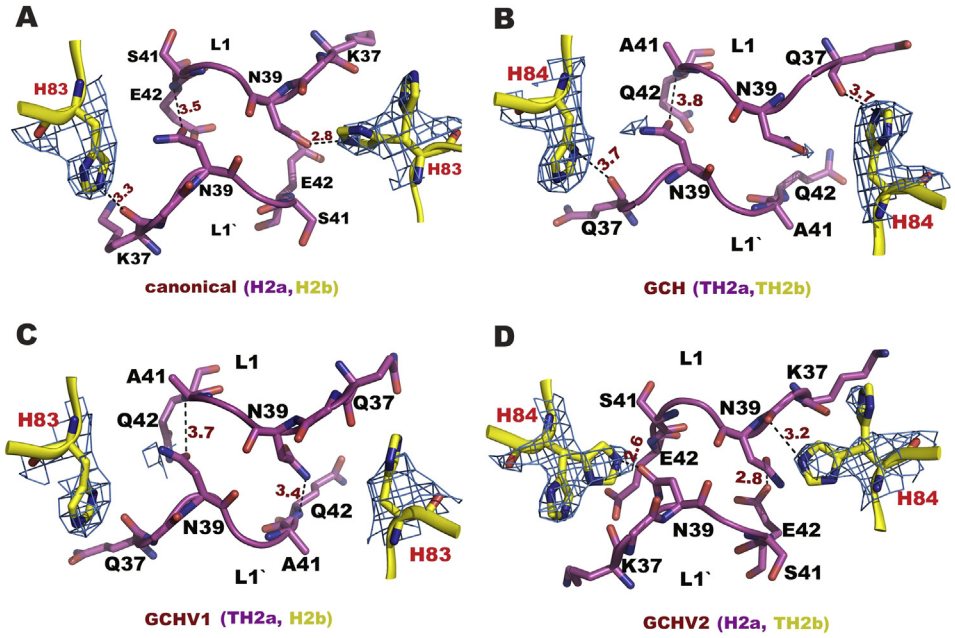

Fig. 3. Close-up views of the L1-L1′ loop interactions within NCPs. A) H2a-H2a′ with H2b (Canonical-NCP). B) TH2a-TH2a′ with TH2b (GCH-NCP), C) TH2a-TH2a′ with H2b (GCHV1-NCP) and D) H2a-H2a′ with TH2b (GCHV2-NCP). The TH2b/H2b-His84/83 residues from both dimers are shown with 2Fo-Fc electron density maps contoured at 1.0σ. The interactions are depicted by dashed black lines.

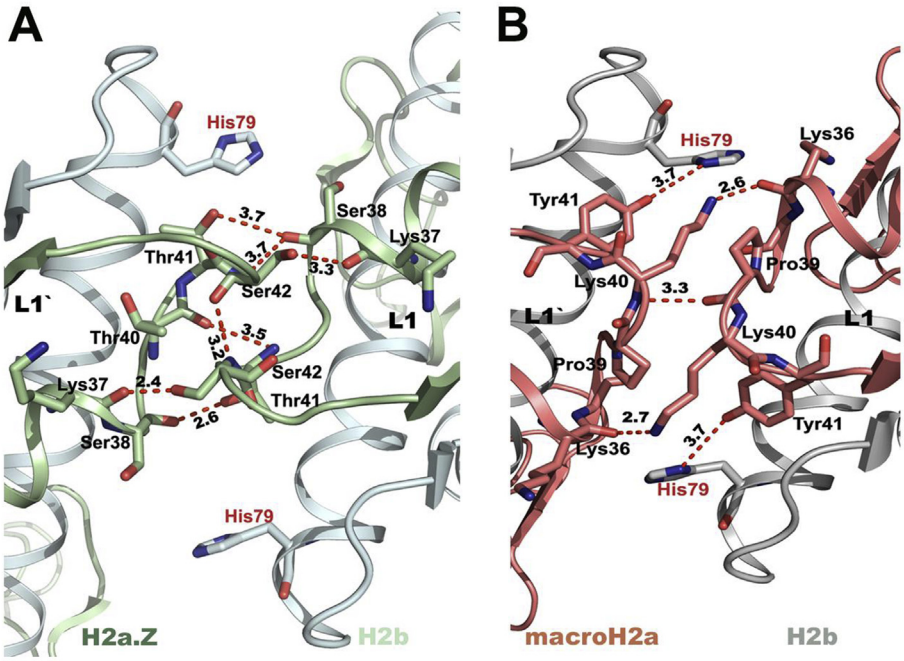

Fig. 4. L1-L1′ loop interactions in H2a variant complexes. A) The H2a.Z-H2a.Z′ interaction (PDB ID: 1F66). B) The macroH2a-macroH2a′ interaction (PDB ID: 1U35). Hydrogen bonds are depicted by dashed red lines and the H2b-His79 residues are marked in red. (For interpretation of the references to colour in this figure legend, the reader is referred to the web version of this article.)

nucleosome entry/exit sites, at a distance of 3.8 Å, and its replacement with Val might affect the above-mentioned interaction (Supplementary Figure S2, B). This loss of interactions will further weaken the strongest histone-DNA interacting region within the NCP, along with the TH2a-Arg21 residue, which might result in the two-fold increase in iPSC generation. It is also interesting to note that both the Glu42 in TH2a and Arg29 in TH2b are critical for iPSC generation in mouse (Supplementary Figure S1), however they are not coserved with other species like human and rat (Supplementary Figure S1) suggesting that these functional residues might be species-specific. Altogether, the above analyses clearly suggested that the loss of the histone dimer-DNA contacts around ±31-bp from the nucleosome entry/exit sites and the modifications in the L1-L1′ interface interactions between TH2a-TH2a′ might have significant impacts on iPSC generation.

Acknowledgments

The authors would like to thank Hiroaki Tachiwana and Hitoshi Kurumizaka for providing the human histone plasmids; Mariko Okada and Viswanathan Thiruselvam for their immense help with protein preparation. The authors are especially grateful to Shigeyuki Yokoyama, Tetsuya Ishikawa, Yoshitsugu Shiro, and Masaki Yamamoto for their moral support, and to the SPring-8 Center for providing funding, in the form of “RSC project for society's needs” for a 3-year period.

Appendix A. Supplementary data

Supplementary data related to this article can be found at http://dx.doi.org/10.1016/j.bbrc.2015.07.070.

References

[1] T. Shinagawa, T. Takagi, D. Tsukamoto, C. Tomaru, L.M. Huynh, P. Sivaraman, T. Kumarevel, K. Inoue, R. Nakato, Y. Katou, T. Sado, S. Takahashi, A. Ogura, K. Shirahige, S. Ishii, Histone variants enriched in oocytes enhance reprogramming to induced pluripotent stem cells, Cell Stem Cell 14 (2014) 217–227.
[2] L.A. Banaszynski, C.D. Allis, P.W. Lewis, Histone variants in metazoan development, Dev. Cell 19 (2010) 662–674.
[3] J. Govin, E. Escoffier, S. Rousseaux, L. Kuhn, M. Ferro, J. Thevenon, R. Catena, I. Davidson, J. Garin, S. Khochbin, C. Caron, Pericentric heterochromatin reprogramming by new histone variants during mouse spermiogenesis, J. cell Biol. 176 (2007) 283–294.
[4] A.K. Shaytan, D. Landsman, A.R. Panchenko, Nucleosome adaptability conferred by sequence and structural variations in histone H2A-H2B dimers, Curr. Opin. Struct. Biol. 32C (2015) 48–57.
[5] Y.C. Choi, C.B. Chae, DNA hypomethylation and germ cell-specific expression of testis-specific H2B histone gene, J. Biol. Chem. 266 (1991) 20504–20511.
[6] I.W. Hwang, K. Lim, C.B. Chae, Characterization of the S-phase-specific transcription regulatory elements in a DNA replication-independent testis-specific H2B (TH2B) histone gene, Mol. Cell. Biol. 10 (1990) 585–592.
[7] R.E. Branson, S.R. Grimes Jr., G. Yonuschot, J.L. Irvin, The histones of rat testis,, Archives Biochem. Biophysics 168 (1975) 403–412.
[8] A. Shires, M.P. Carpenter, R. Chalkley, New histones found in mature mammalian testes, Proc. Natl. Acad. Sci. U. S. A. 72 (1975) 2714–2718.
[9] N.E. Huh, I.W. Hwang, K. Lim, K.H. You, C.B. Chae, Presence of a bi-directional S phase-specific transcription regulatory element in the promoter shared by testis-specific TH2A and TH2B histone genes, Nucleic Acids Res. 19 (1991) 93–98.
[10] J. Jullien, V. Pasque, R.P. Halley-Stott, K. Miyamoto, J.B. Gurdon, Mechanisms of nuclear reprogramming by eggs and oocytes: a deterministic process?, Nature reviews, Mol. Cell Biol. 12 (2011) 453–459.
[11] S. Yamanaka, H.M. Blau, Nuclear reprogramming to a pluripotent state by three approaches, Nature 465 (2010) 704–712.
[12] J.B. Gurdon, T.R. Elsdale, M. Fischberg, Sexually mature individuals of Xenopus laevis from the transplantation of single somatic nuclei, Nature 182 (1958) 64–65.
[13] C.A. Cowan, J. Atienza, D.A. Melton, K. Eggan, Nuclear reprogramming of somatic cells after fusion with human embryonic stem cells, Science 309 (2005) 1369–1373.
[14] K. Takahashi, S. Yamanaka, Induction of pluripotent stem cells from mouse embryonic and adult fibroblast cultures by defined factors, Cell 126 (2006) 663–676.
[15] A. Philpott, G.H. Leno, R.A. Laskey, Sperm decondensation in Xenopus egg cytoplasm is mediated by nucleoplasmin, Cell 65 (1991) 569–578.
[16] S. Banuelos, M.J. Omaetxebarria, I. Ramos, M.R. Larsen, I. Arregi, O.N. Jensen, J.M. Arizmendi, A. Prado, A. Muga, Phosphorylation of both nucleoplasmin domains is required for activation of its chromatin decondensation activity, J. Biol. Chem. 282 (2007) 21213–21221.
[17] R.T. Kamakaka, S. Biggins, Histone variants: deviants? Genes & Dev. 19 (2005) 295–310.
[18] Y. Tanaka, M. Tawaramoto-Sasanuma, S. Kawaguchi, T. Ohta, K. Yoda, H. Kurumizaka, S. Yokoyama, Expression and purification of recombinant human histones, Methods 33 (2004) 3–11.
[19] K. Luger, T.J. Rechsteiner, T.J. Richmond, Preparation of nucleosome core particle from recombinant histones, Methods Enzym. 304 (1999) 3–19.
[20] P.N. Dyer, R.S. Edayathumangalam, C.L. White, Y. Bao, S. Chakravarthy, U.M. Muthurajan, K. Luger, Reconstitution of nucleosome core particles from recombinant histones and DNA, Methods Enzym. 375 (2004) 23–44.
[21] K. Luger, A.W. Mader, R.K. Richmond, D.F. Sargent, T.J. Richmond, Crystal structure of the nucleosome core particle at 2.8 A resolution, Nature 389 (1997) 251–260.
[22] G.N. Murshudov, A.A. Vagin, E.J. Dodson, Refinement of macromolecular structures by the maximum-likelihood method, Acta crystallographica. Section D, Biol. Crystallogr. 53 (1997) 240–255.
[23] A.T. Brunger, Version 1.2 of the Crystallography and NMR system, Nat. Protoc. 2 (2007) 2728–2733.
[24] P. Emsley, K. Cowtan, Coot: model-building tools for molecular graphics, Acta crystallographica. Section D, Biol. Crystallogr. 60 (2004) 2126–2132.
[25] H. Tachiwana, W. Kagawa, A. Osakabe, K. Kawaguchi, T. Shiga, Y. Hayashi-Takanaka, H. Kimura, H. Kurumizaka, Structural basis of instability of the nucleosome containing a testis-specific histone variant, human H3T, Proc. Natl. Acad. Sci. U. S. A. 107 (2010) 10454–10459.
[26] T. Urahama, N. Horikoshi, A. Osakabe, H. Tachiwana, H. Kurumizaka, Structure of human nucleosome containing the testis-specific histone variant TSH2B, Acta crystallographica. Section F, Struct. Biol. Commun. 70 (2014) 444–449.
[27] M.A. Hall, A. Shundrovsky, L. Bai, R.M. Fulbright, J.T. Lis, M.D. Wang, High-resolution dynamic mapping of histone-DNA interactions in a nucleosome, Nat. Struct. Mol. Biol. 16 (2009) 124–129.
[28] A. Li, A.H. Maffey, W.D. Abbott, N. Conde e Silva, A. Prunell, J. Siino, D. Churikov, A.O. Zalensky, J. Ausio, Characterization of nucleosomes consisting of the human testis/sperm-specific histone H2B variant (hTSH2B), Biochemistry 44 (2005) 2529–2535.
[29] E. Montellier, F. Boussouar, S. Rousseaux, K. Zhang, T. Buchou, F. Fenaille, H. Shiota, A. Debernardi, P. Hery, S. Curtet, M. Jamshidikia, S. Barral, H. Holota, A. Bergon, F. Lopez, P. Guardiola, K. Pernet, J. Imbert, C. Petosa, M. Tan, Y. Zhao, M. Gerard, S. Khochbin, Chromatin-to-nucleoprotamine transition is controlled by the histone H2B variant TH2B, Genes & Dev. 27 (2013) 1680–1692.
[30] T. Shinagawa, L.M. Huynh, T. Takagi, D. Tsukamoto, C. Tomaru, H.G. Kwak, N. Dohmae, J. Noguchi, S. Ishii, Disruption of Th2a and Th2b genes causes defects in spermatogenesis, Development 142 (2015) 1287–1292.
[31] U.M. Muthurajan, Y. Bao, L.J. Forsberg, R.S. Edayathumangalam, P.N. Dyer, C.L. White, K. Luger, Crystal structures of histone Sin mutant nucleosomes reveal altered protein-DNA interactions, EMBO J. 23 (2004) 260–271.
[32] H. Tachiwana, W. Kagawa, T. Shiga, A. Osakabe, Y. Miya, K. Saito, Y. Hayashi-Takanaka, T. Oda, M. Sato, S.Y. Park, H. Kimura, H. Kurumizaka, Crystal structure of the human centromeric nucleosome containing CENP-A, Nature 476 (2011) 232–235.
[33] C. Bonisch, S.B. Hake, Histone H2A variants in nucleosomes and chromatin: more or less stable? Nucleic Acids Res. 40 (2012) 10719–10741.
[34] S. Chakravarthy, S.K. Gundimella, C. Caron, P.Y. Perche, J.R. Pehrson, S. Khochbin, K. Luger, Structural characterization of the histone variant macroH2A, Mol. Cell. Biol. 25 (2005) 7616–7624.
[35] R.K. Suto, M.J. Clarkson, D.J. Tremethick, K. Luger, Crystal structure of a nucleosome core particle containing the variant histone H2A.Z, Nat. Struct. Biol. 7 (2000) 1121–1124.
[36] S.D. Taverna, H. Li, A.J. Ruthenburg, C.D. Allis, D.J. Patel, How chromatin-binding modules interpret histone modifications: lessons from professional pocket pickers, Nat. Struct. Mol. Biol. 14 (2007) 1025–1040.
[37] J. Allan, N. Harborne, D.C. Rau, H. Gould, Participation of core histone “tails” in the stabilization of the chromatin solenoid, J. Cell Biol. 93 (1982) 285–297.
[38] W.L. Cheung, K. Ajiro, K. Samejima, M. Kloc, P. Cheung, C.A. Mizzen, A. Beeser, L.D. Etkin, J. Chernoff, W.C. Earnshaw, C.D. Allis, Apoptotic phosphorylation of histone H2B is mediated by mammalian sterile twenty kinase, Cell 113 (2003) 507–517.
[39] T. Hagiwara, Y. Hidaka, M. Yamada, Deimination of histone H2A and H4 at arginine 3 in HL-60 granulocytes, Biochemistry 44 (2005) 5827–5834.
[40] A.E. de la Barre, D. Angelov, A. Molla, S. Dimitrov, The N-terminus of histone H2B, but not that of histone H3 or its phosphorylation, is essential for chromosome condensation,, EMBO J. 20 (2001) 6383–6393.
[41] N. Mosammaparast, K.R. Jackson, Y. Guo, C.J. Brame, J. Shabanowitz, D.F. Hunt, L.F. Pemberton, Nuclear import of histone H2A and H2B is mediated by a network of karyopherins, J. cell Biol. 153 (2001) 251–262.
[42] A. Jamai, R.M. Imoberdorf, M. Strubin, Continuous histone H2B and transcription-dependent histone H3 exchange in yeast cells outside of replication, Mol. Cell 25 (2007) 345–355.